Safety-Critical Control of Autonomous Surface Vehicles in the Presence of Ocean Currents

Erlend A. Basso, Emil H. Thyri, Kristin Y. Pettersen, Morten Breivik, and Roger Skjetne

***Abstract*— Autonomous surface vehicles (ASVs) are safety-critical systems that must provide strict safety guarantees such as collision avoidance to enable fully autonomous operations. This paper presents a unified framework for safety-critical control of ASVs for maneuvering, dynamic positioning, and control allocation with safety guarantees in the presence of unknown ocean currents. The framework utilizes control Lyapunov function (CLF)- and control barrier function (CBF)-based quadratic programs (QPs), and is applicable to a general class of nonlinear affine control systems. The stabilization objective is formulated as a maneuvering problem and integral action is introduced in the CLFs to counteract the effect of unknown irrotational ocean currents. Furthermore, ocean current estimates are constructed for robust CBF design, and analytic conditions under which the estimates guarantee safety are derived. Subsequently, robust CBFs are designed to achieve collision avoidance of static obstacles. The paper concludes by verifying the framework in simulation for a double-ended passenger ferry.**

I. Introduction

In recent years, a significant research effort has been devoted to autonomous surface vehicles (ASVs). Fully autonomous surface vehicles will have a significant impact in a wide variety of areas such as commercial shipping [1], passenger transport [2], scientific research [3], and military applications. ASVs are safety-critical systems with a tight coupling between the potentially conflicting maneuvering objectives (e.g. following a geometric path at a desired speed), and safety-related objectives such as collision avoidance. The control problem is further complicated by magnitude and rate constraints on the actuators, and nonlinear actuator models in the case of azimuth thrusters.

Control algorithms for marine vessels often decouple the control problem into two parts. First, a high-level motion control algorithm is developed for position and heading control by considering the forces and moments generated by the actuators as a virtual control input. After determining the virtual control input from the motion control algorithm, a control allocation problem must be solved in order to distribute the virtual control input into the physical control inputs of the actuators such that the total forces and moments generated by the actuators correspond to the virtual input. This decoupling is not very restrictive for systems where the actuator configuration is constant. However, for actuators such as azimuth thrusters, the azimuth angles are also control inputs, and a nonlinear control allocation problem must be solved, requiring sophisticated real-time optimization techniques [4], [5].

Decoupling the control problem makes it difficult to account for magnitude and rate constraints within the motion control algorithm, which can lead to virtual control inputs from the motion control algorithm that cannot be realized by the actuator control inputs. The actuator control inputs must then be found by minimizing the difference between the virtual control input and the total forces and moments generated by the actuators in some sense. A drawback of this approach is the fact that this minimization does not necessarily lead to minimizing the tracking error.

Control allocation algorithms for systems with linear and nonlinear actuator models were surveyed in [6]. In [7], a model predictive control algorithm combined position and heading control with control allocation for a dynamic positioning application. This approach requires a linear model and is less feasible for marine vessels operating at higher speeds, where centripetal forces and nonlinear damping effects dominate.

Control Lyapunov function (CLF)-based quadratic programs (QP) have been applied to a variety of systems including biped robots [8]–[11], automotive systems [12], and hyper-redundant underwater manipulators [13]. CLF-based QP controllers are attractive due to their real-time feasibility on standard hardware [14] and natural inclusion of actuator magnitude and rate constraints. Gradual performance degradation of a CLF-based QP controller under strict input constraints was experimentally shown in [10]. While CLFs thus are attractive for achieving the maneuvering objectives of ASVs, control barrier functions (CBFs) are a powerful tool for ensuring forward invariance of sets in order to provide safety guarantees. CBFs were introduced in [15] and unified with CLFs in [16] and [12] using different formulations. This paper builds on the approach taken in [12], which mediated safety and stabilization objectives by guaranteeing safety and achieving stabilization when the objectives are not in conflict. CBFs have been utilized for collision avoidance of miniature differential drive robots in [17], [18], underwater manipulators [13], and recently for ASVs in [19]. A method for robust CLF-CBF-QP control was proposed in [11], which achieves robustness through constant scalar-valued upper bounds on the model uncertainty appearing in the CLF and CBF derivatives, often leading to overly conservative estimates. Robust CBFs for uncertain systems were also considered in [20] and [18]. The method in [20] results in a nonlinear optimization problem, making it less feasible for real-time applications, while [18] extended CBFs to a particular class of disturbed

This work was supported by the Research Council of Norway through the Centres of Excellence funding scheme, project no. 223254 - NTNU AMOS

The authors are with the Centre for Autonomous Marine Operations and Systems (NTNU AMOS), Norwegian University of Science and Technology, NO-7491 Trondheim, Norway {erlend.a.basso, emil.h.thyri, kristin.y.pettersen, roger.skjetne}@ntnu.no, morten.breivik@ieee.org

systems modeled by differential inclusions.

In this paper we propose a CLF- and CBF-based convex quadratic optimization problem for robust safety-critical control of ASVs. The framework builds on [8], [12], [18], [21], and is applicable to a larger class of nonlinear affine control systems. Safety-related objectives are enforced through CBFs, while stabilization objectives are enforced through relaxed CLFs. Relaxation of the CLFs implies that the stabilization and safety-related objectives do not need to be simultaneously satisfiable. We propose CLFs endowed with integral action in order to mitigate the effects of unknown and slowly varying nonlinearities such as the effect of ocean currents. Moreover, we modify the results on robust CBFs in [18] for uncertain systems modeled by differential equations in order to provide analytical conditions guaranteeing safety in the presence of unknown nonlinearities. These conditions are subsequently utilized to obtain robust CBFs ensuring reactive collision avoidance for ASVs. Employing an optimization-based control law enables formulating the control problem in terms of the actuator control inputs and thereby unifying the control problem with the control allocation problem. This unification handles control input saturations more effectively than a decoupled approach and is less likely to lead to instability [10], which is especially relevant during emergency collision avoidance maneuvers. We consider ASVs with nonlinear actuator models and derive a partially linearized control design model by linearizing the actuator configuration matrix at every time step to avoid a non-convex optimization problem.

This paper is organized as follows, Section II presents background theory on CLFs and CBFs before we derive conditions guaranteeing safety in the presence of unknown nonlinearities. These conditions are subsequently employed for safe CLF-CBF-QP controller synthesis for a general nonlinear affine control system. In Section III, ASV models for simulation, and CLF and CBF design in the presence of unknown ocean currents are presented. For CBF design, an arbitrary number of ocean current approximations are generated and conditions guaranteeing safety are derived. Section IV introduces the stabilization objective before we construct CLFs with integral action and robust CBFs for reactive collision avoidance. Moreover, a general CLF-CBF-QP controller for safety-critical control is presented. A simulation study for a double-ended passenger ferry implements the proposed framework in Section V, before Section VI concludes the paper.

II. Safety-Critical Control of Nonlinear Affine Control Systems

This section presents background theory on CLFs and CBFs before the main theoretical result of this paper is presented in Theorem 2. Specifically, Theorem 2 provides conditions for which an arbitrary number of nonlinear maps estimating some unknown system nonlinearity guarantees safety. Section II-C extends the CLF-CBF-QP controller from [12] by using Theorem 2 to guarantee safety in the presence of unknown nonlinearities and by incorporating CLFs with integral action to remove steady-state tracking errors.

A. Preliminaries on CLFs and CBFs

Consider the nonlinear control affine system

$$\dot{\chi} = f(\chi) + g(\chi)u, \tag{1}$$

where $\chi \in \mathbb{R}^d$, the mappings $f\colon \mathbb{R}^d \to \mathbb{R}^d$ and $g\colon \mathbb{R}^d \to \mathbb{R}^{d\times p}$ are locally Lipschitz and $u \in \mathcal{U} \subset \mathbb{R}^p$, where the input space $\mathcal{U}$ is nonempty, closed and convex.

CLFs are continuously differentiable and positive definite functions whose time derivatives can be made negative definite by appropriate selection of the control input. Exponentially stabilizing CLFs achieve convergence rates within explicitly given bounds, and provides an inherent robustness property to disturbances, in terms of input-to-state stability.

Definition 1 (Definition 1. [9])**.** *For the system* (1)*, a continuously differentiable function $V : \mathbb{R}^d \to \mathbb{R}$ is an exponentially stabilizing control Lyapunov function (ES-CLF) if there exists positive constants $c_1, c_2, c_3 > 0$ such that*

$$c_1\|\chi\|^2 \leq V(\chi) \leq c_2\|\chi\|^2, \tag{2}$$

$$\inf_{u\in\mathcal{U}} \left[\frac{\partial V}{\partial \chi} f(\chi, t) + \frac{\partial V}{\partial \chi} g(\chi)u + c_3 V(\chi)\right] \leq 0, \tag{3}$$

for all $\chi \in \mathbb{R}^d$.

Safety-related objectives are often described by inequalities or sets. Control barrier functions are continuously differentiable functions $h : \mathbb{R}^d \to \mathbb{R}$ for which the super-zero level set

$$\mathcal{C} = \left\{\chi \in \mathbb{R}^d : h(\chi) \geq 0\right\}, \tag{4}$$

can be rendered forward invariant by appropriate selection of the control input [22].

Definition 2 (Definition 2. [22])**.** *Let $\mathcal{C} \subset \mathbb{R}^d$ be the super-zero level set of a continuously differentiable function $h : \mathbb{R}^d \to \mathbb{R}$, then h is a control barrier function (CBF) for the system* (1) *if there exists an extended class $\mathcal{K}_\infty$ function σ such that*

$$\sup_{u\in\mathcal{U}} \left[\frac{\partial h}{\partial \chi} f(\chi) + \frac{\partial h}{\partial \chi} g(\chi)u\right] \geq -\sigma\left(h(\chi)\right), \tag{5}$$

for all $\chi \in \mathbb{R}^d$.

Theorem 1 (Theorem 2. [22])**.** *Let $\mathcal{C} \subset \mathbb{R}^d$ be a set defined as the super-zero level set of a continuously differentiable function $h\colon \mathbb{R}^d \to \mathbb{R}$. If h is a control barrier function on $\mathbb{R}^d$ and $\frac{\partial h}{\partial \chi} \neq 0$ for all $\chi \in \partial C = \left\{\chi \in \mathbb{R}^d\colon h(\chi) = 0\right\}$, then any Lipschitz continuous control law*

$$u(\chi) \in \left\{u \in \mathcal{U}\colon \frac{\partial h}{\partial \chi} f(\chi) + \frac{\partial h}{\partial \chi} g(\chi)u + \sigma(h(\chi)) \geq 0\right\}, \tag{6}$$

for the system (1) *renders the set $\mathcal{C}$ forward invariant. Additionally, the set $\mathcal{C}$ is asymptotically stable.*

B. Robust CBFs for a Class of Uncertain Nonlinear Systems

Assume that $f(\chi) = \tilde{f}(\chi) + \vartheta(\chi)$ and rewrite (1) as

$$\dot{\chi} = \tilde{f}(\chi) + \vartheta(\chi) + g(\chi)u, \tag{7}$$

where the unknown mapping $\vartheta : \mathbb{R}^d \to \mathbb{R}^d$ is locally Lipschitz. We modify the robustness results for disturbed nonlinear

affine control systems described by set-valued maps in [18] to the system (7) as follows:

Theorem 2. *Consider $P > 0$ continuous maps $\varphi_i : \mathbb{R}^d \to \mathbb{R}^d$, $i \in \mathcal{P} = \{1, \dots, P\}$, and let $h : \mathbb{R}^d \to \mathbb{R}$ be a continuously differentiable function. If the mappings φ_i satisfy*

$$\min_{i \in \mathcal{P}} \frac{\partial h}{\partial \chi} \varphi_i(\chi) \leq \frac{\partial h}{\partial \chi} \vartheta(\chi), \tag{8}$$

for all $\chi \in \mathbb{R}^d$, and if there exists a Lipschitz continuous control law $u \colon \mathbb{R}^d \to \mathbb{R}^p$ and an extended class-$\mathcal{K}_\infty$ function $\sigma \colon \mathbb{R} \to \mathbb{R}$ such that

$$\frac{\partial h}{\partial \chi} \tilde{f}(\chi) + \frac{\partial h}{\partial \chi} g(\chi) u \geq -\sigma(h(\chi)) - \min_{i \in \mathcal{P}} \frac{\partial h}{\partial \chi} \varphi_i(\chi), \tag{9}$$

for all $\chi \in \mathbb{R}^d$, then h is a CBF for (7) and the control law $u(\chi)$ renders the super-zero level set $\mathcal{C}$ forward invariant if $\frac{\partial h}{\partial \chi} \neq 0$ when $\chi \in \partial \mathcal{C}$.

Proof. The proof follows from the fact that $\tilde{f}(\chi)$ and $g(\chi)$ are locally Lipschitz, the minimum of continuous maps is in itself continuous, and by combining (8) with (9)

$$\frac{\partial h}{\partial \chi} \tilde{f}(\chi) + \frac{\partial h}{\partial \chi} g(\chi) u \geq -\sigma(h(\chi)) - \frac{\partial h}{\partial \chi} \vartheta(\chi), \tag{10}$$

which is equivalent to

$$\frac{\partial h}{\partial \chi} f(\chi) + \frac{\partial h}{\partial \chi} g(\chi) u(\chi) \geq -\sigma(h(\chi)), \tag{11}$$

for all $\chi \in \mathbb{R}^d$. By Definition 2, h is a valid CBF for (7), which combined with the fact that $u(\chi)$ is Lipschitz continuous and $\frac{\partial h}{\partial \chi} \neq 0$ when $\chi \in \partial \mathcal{C}$, guarantees forward invariance of the super-zero level set $\mathcal{C}$ from Theorem 1. □

Theorem 2 can be used to synthesize safe controllers by generating P continuous maps capturing the unknown nonlinearity with sufficient accuracy. By enforcing (9) as a constraint on the control input, the effect of the most conservative function estimate $\varphi_i(\chi)$ on the positivity of the function $h(\chi)$ can be accounted for. Moreover, by constructing state-dependent function estimates we can avoid excessively conservative scalar estimates on the norm of the uncertain term $\frac{\partial h}{\partial \chi} \vartheta(\chi)$ as in [11].

C. Controller Synthesis via Quadratic Programming

If the unknown mapping ϑ is slowly varying, it is reasonable to assume that an ES-CLF $V(\chi)$ with integral action for the system (7) with $\vartheta = 0$ will stabilize (1). Moreover, consider a safety-related objective encoded by $h(\chi)$. By relaxing the stabilization objective, a safe controller can be synthesized for the system (1) by solving the following QP

$$\underset{(u,\delta) \in \mathbb{R}^{p+1}}{\text{minimize}} \quad \frac{1}{2} u^\mathsf{T} H u + c^\mathsf{T} u + w\delta^2 \tag{12a}$$

subject to

$$\frac{\partial V}{\partial \chi} \tilde{f}(\chi) + \frac{\partial V}{\partial \chi} g(\chi) u \leq -\gamma V(\chi) + \delta, \tag{12b}$$

$$\frac{\partial h}{\partial \chi} \tilde{f}(\chi) + \frac{\partial h}{\partial \chi} g(\chi) u \geq -\sigma(h(\chi)) - \min_{i \in \mathcal{P}} \frac{\partial h}{\partial \chi} \varphi_i(\chi), \tag{12c}$$

where $H \in \mathbb{R}^{p \times p}$ is any positive definite matrix, $c \in \mathbb{R}^{p+1}$, and $\delta \in \mathbb{R}$ is a slack variable penalized by the weighting parameter $w > 0$. The slack variable is added to ensure feasibility of the optimization problem in case the stabilization objective conflicts with the safety-related objective. Moreover, the addition of the slack variable ensures that the safety-related objective can always be satisfied. By choosing the weighting parameter appropriately, the solution to the QP will result in $\delta \approx 0$ when the stabilization and safety-related objectives are not conflicting. Furthermore, by assuming that each $\varphi_i(x)$ and the gradients of h and V are locally Lipschitz, the solution to (12) is locally Lipschitz continuous for all $\chi \in \mathbb{R}^d$ such that $h(\chi) > 0$ [21].

III. Vessel Modeling for Safety and Stabilization

This section presents ASV models for stabilization and safety design. Specifically, in Sections III-A and III-B we describe the simulation model and the control allocation problem. The control design model, which does not include the effect of the unknown ocean currents, is presented in Section III-C. Moreover, we formulate the model in terms of the azimuth angle and force magnitude control inputs of the actuators, and not the generalized forces produced by the actuators. This allows us to subsequently linearize the mapping from control inputs to generalized forces, avoiding a non-convex dynamic optimization problem. In Section III-D we consider the validity of the control design model and modify it accordingly for CBF design. Furthermore, we modify Theorem 2 to the case where the unknown map ϑ is known, but depends on an unknown vector of parameters, which enables safe controller synthesis in the presence of unknown ocean currents.

A. Vessel Model

The system configuration of a surface vessel can be described by $\eta = \operatorname{col}(p^n, \psi)$, where $p^n = \operatorname{col}(x^n, y^n) \in \mathbb{R}^2$ is the North and East coordinates of the body frame of the ship in the assumed inertial North-East-Down (NED) frame, and $\psi \in D_\psi = (-\pi, \pi] \subset \mathbb{R}$ is the heading angle. Let the rotation matrix $R : D_\psi \to \mathrm{SO}(3)$ describe the rotation between the body frame and NED frame, and define the generalized velocity vector expressed in the body frame by $\nu := \operatorname{col}(u, v, r) \in \mathbb{R}^3$.

Assumption 1. *The unknown ocean current V_c is defined in the NED frame, and is assumed to be constant and irrotational. Hence, $V_c = U_c \operatorname{col}(\cos(\beta_c), \sin(\beta_c), 0)$, where $\beta_c \in (-\pi, \pi]$ is the current direction and $U_c \geq 0$ is the current speed.*

Assumption 1 implies that the ocean current in the body frame is given by $\nu_c = \operatorname{col}(u_c, v_c, 0) = R^\mathsf{T}(\psi) V_c$, with $\dot{\nu}_c = \operatorname{col}(r v_c, -r u_c, 0) = \dot{R}^\mathsf{T} V_c$. Defining the relative velocity by $\nu_r := \nu - \nu_c$, the equations of motion are given by [23]

$$\dot{\eta} = R(\psi)\nu, \tag{13a}$$

$$\dot{\nu} = \dot{R}^\mathsf{T}(\psi, r) V_c + M^{-1} \left(\tau - C(\nu_r)\nu_r - D(\nu_r)\nu_r \right), \tag{13b}$$

where M is the inertia matrix including hydrodynamic added mass, $C(\nu_r)$ is the Coriolis-centripetal matrix including hydrodynamic added mass, $D(\nu_r)$ is the damping matrix, and

$\tau \in \mathbb{R}^3$ are the generalized forces produced by the actuators. Moreover, the Coriolis and centripetal matrix can be expressed as $C(\nu_r) = C(\nu) + \bar{C}(\nu_c)$, while the damping matrix can be decomposed into a linear and nonlinear part $D(\nu_r) = D_l + D_n(\nu_r)$, where

$$D_n(\nu_r) = -\begin{bmatrix} d_1|u_r| & 0 & 0 \\ 0 & d_2|v_r| + d_3|r| & d_4|v_r| + d_5|r| \\ 0 & d_6|v_r| + d_7|r| & d_8|v_r| + d_9|r| \end{bmatrix}, \quad (14)$$

where $d_j \in \mathbb{R}$, $j \in \{1, \ldots, 9\}$. See [23] for further details.

B. Control Allocation

Consider a marine vessel equipped with m actuators, the mapping between the generalized forces τ and the control inputs $u = \operatorname{col}(\mu, \alpha) \in \mathbb{R}^{2m}$ is given by

$$\tau = B(\alpha)\mu, \quad (15)$$

where $B : \mathbb{R}^m \to \mathbb{R}^{3\times m}$ is the actuator configuration matrix, α are the azimuth angles of the actuators and μ is the vector of force magnitudes produced by the actuators. The ith column of the actuator configuration matrix is given by

$$B_i(\alpha_i) = \begin{bmatrix} \cos\alpha_i \\ \sin\alpha_i \\ -l_{y_i}\cos\alpha_i + l_{x_i}\sin\alpha_i \end{bmatrix}, \quad (16)$$

where the location of the ith actuator in a body-fixed coordinate system with origin at the center of rotation is at $\operatorname{col}(l_{x_i}, l_{y_i})$. Solving (15) for the actuator control inputs μ, α, given a desired generalized force τ, is known as the control allocation problem [4].

C. Vessel Model for CLF-based Control Design

For low-speed maneuvering up to $2\,\mathrm{m/s}$, linear damping is the dominating dissipative force [23]. Moreover, from (14) it is apparent that approximating $D_n(\nu_r)$ by $D_n(\nu)$ is ill-advised when the vessel and current velocity are similar in magnitude and the current direction is unknown. Therefore, we simplify the model (13) for control design by by neglecting the effects of nonlinear damping and by assuming that $V_c = 0$

$$\dot{\eta} = R(\psi)\nu, \quad (17a)$$
$$M\dot{\nu} + C(\nu)\nu + D_l\nu = B(\alpha)\mu, \quad (17b)$$

where $u = \operatorname{col}(\mu, \alpha) \in \mathbb{R}^{2m}$ is the control input. Since the system (17) is not affine in the control input u, the design procedure in Section II will yield a non-convex dynamic optimization problem due to the resulting non-convexity of (12b) and (12c). Following [4], a control affine system is obtained by linearizing (15) about the azimuth angles α_0 and force magnitudes μ_0 from the previous sample

$$\begin{aligned} B(\alpha)\mu &\approx B(\alpha_0)\Delta\mu + \frac{\partial}{\partial\alpha}\left(B(\alpha)\mu\right)\Big|_{\substack{\alpha=\alpha_0 \\ \mu=\mu_0}} \Delta\alpha + B(\alpha_0)\mu_0 \\ &= \underbrace{\begin{bmatrix} B(\alpha_0) & \frac{\partial}{\partial\alpha}\left(B(\alpha)\mu\right)\big|_{\substack{\alpha=\alpha_0 \\ \mu=\mu_0}} \end{bmatrix}}_{\bar{B}(\alpha_0,\mu_0)} \Delta u + B(\alpha_0)\mu_0, \quad (18) \end{aligned}$$

where $\Delta\mu = \mu - \mu_0$, $\Delta\alpha = \alpha - \alpha_0$ and $\Delta u = u - u_0 = \operatorname{col}(\Delta\mu, \Delta\alpha)$. Combining (18) and (17) yields the partially linearized control affine system

$$\dot{\eta} = R(\psi)\nu, \quad (19a)$$
$$M\dot{\nu} + C(\nu)\nu + D_l\nu = \bar{B}(u_0)\Delta u + B(\alpha_0)\mu_0. \quad (19b)$$

which admits the following state-space representation

$$\dot{x} = f(x) + g\Delta u, \quad (20)$$

where $x = \operatorname{col}(\eta, \nu)$ and

$$f(x) = \begin{bmatrix} R(x_1)x_2 \\ M^{-1}\left(B(\alpha_0)\mu_0 - C(x_2)x_2 - D_l x_2\right) \end{bmatrix}, \quad (21)$$

$$g = \begin{bmatrix} 0_{3\times 2m} \\ M^{-1}\bar{B}(\alpha_0, \mu_0) \end{bmatrix}. \quad (22)$$

D. Vessel Model for CBF Design

Under the assumption that the dynamics related to the current and other unmodeled dynamics are captured by a slowly varying bias, experience has shown that the model (19) is sufficiently precise for control design provided that integral action is used in the controller [23], [24]. For CBF design, we assume low-speed maneuvering and modify the full model (13) by neglecting nonlinear damping

$$\dot{\eta} = R(\psi)\nu, \quad (23a)$$
$$\dot{\nu} = M^{-1}\left(\tau(\eta, \nu) - C(\nu)\nu - D_l\nu\right) + \vartheta(\psi, r, \nu, \nu_c), \quad (23b)$$

where

$$\vartheta = \dot{R}^{\mathsf{T}}(\psi, r)V_c + M^{-1}\left(C(\nu)\nu_c - \bar{C}(\nu_c)\nu_r + D_l\nu_c\right). \quad (24)$$

The system (23) has the following state-space representation

$$\dot{x} = \breve{f}(x, \nu_c) + \breve{g}\tau(x), \quad (25)$$

where $x = \operatorname{col}(\eta, \nu)$ and

$$\breve{f}(x, \nu_c) = f(x) + \begin{bmatrix} 0_{3\times 1} \\ \vartheta(x, \nu_c) \end{bmatrix}, \quad \breve{g} = \begin{bmatrix} 0_{3\times 3} \\ M^{-1} \end{bmatrix}, \quad (26)$$

where $\breve{f}\colon \mathbb{R}^2 \times D_\psi \times \mathbb{R}^3 \times \mathbb{R}^3 \to \mathbb{R}^6$ and $\breve{g} \in \mathbb{R}^{6\times 3}$ are locally Lipschitz. We want to generate $P > 0$ continuous maps approximating the dynamic effect of the ocean current. To this end, Theorem 2 is specialized for the case where the mapping ϑ is known, but instead depends on the unknown parameters ν_c.

Proposition 1. *Given $P > 0$ ocean current estimates $\hat{V}_{c,i}$, $i \in \mathcal{P} = \{1, \ldots, P\}$, define P continuous maps $\varphi_i\colon D_\psi \times \mathbb{R} \times \mathbb{R}^3 \times \mathbb{R}^3 \to \mathbb{R}^3$ by*

$$\begin{aligned} \varphi_i(\psi, r, \nu, \hat{\nu}_{c,i}) &:= \dot{R}^{\mathsf{T}}(\psi, r)\hat{V}_{c,i} \\ &\quad + M^{-1}\left(C(\nu)\hat{\nu}_{c,i} - \bar{C}(\hat{\nu}_{c,i})\hat{\nu}_{r,i} + D_l\hat{\nu}_{c,i}\right), \end{aligned} \quad (27)$$

where $\hat{\nu}_{c,i} = R^{\mathsf{T}}(\psi)\hat{V}_{c,i}$ and $\hat{\nu}_{r,i} = \nu - \hat{\nu}_{c,i}$. Let $h : \mathbb{R}^2 \times D_\psi \times \mathbb{R}^3 \to \mathbb{R}$ be a continuously differentiable function. If the ocean current estimates $\hat{\nu}_{c,i}$ satisfy

$$\min_{i\in\mathcal{P}} \frac{\partial h}{\partial \nu}\varphi_i(\psi, r, \nu, \hat{\nu}_{c,i}) \le \frac{\partial h}{\partial \nu}\vartheta(\psi, r, \nu, \nu_c), \quad (28)$$

for all $(\eta, \nu) \in \mathbb{R}^2 \times D_\psi \times \mathbb{R}^3$ *and if there exists a Lipschitz continuous control law* $\tau \colon \mathbb{R}^2 \times D_\psi \times \mathbb{R}^3 \to \mathbb{R}^3$ *and an extended class-*$\mathcal{K}_\infty$ *function* $\sigma \colon \mathbb{R} \to \mathbb{R}$ *such that*

$$\begin{aligned} &\frac{\partial h}{\partial \eta} R(\psi)\nu + \frac{\partial h}{\partial \nu} M^{-1}\left(\tau(\eta,\nu) - C(\nu)\nu - D_l\nu\right) \\ &\geq -\sigma(h) - \min_{i \in \mathcal{P}} \frac{\partial h}{\partial \nu} \varphi_i(\psi, r, \nu, \hat{\nu}_{c,i}), \end{aligned} \tag{29}$$

for all $(\eta, \nu) \in \mathbb{R}^2 \times D_\psi \times \mathbb{R}^3$*, then* h *is a CBF for* (23) *and the control law* $\tau(\eta, \nu)$ *renders the super-zero level set* $\mathcal{C}$ *forward invariant if* $\frac{\partial h}{\partial \nu} \neq 0$ *when* $(\eta, \nu) \in \partial\mathcal{C}$*.*

Proof. The proof follows from noting that $\breve{f}(x, \nu_c)$ and $\breve{g}$ are locally Lipschitz, the minimum of continuous maps is in itself continuous, and by combining (28) with (29)

$$\begin{aligned} &\frac{\partial h}{\partial \eta} R(\psi)\nu + \frac{\partial h}{\partial \nu} M^{-1}\left(\tau(\eta,\nu) - C(\nu)\nu - D_l\nu\right) \\ &\geq -\sigma(h) - \frac{\partial h}{\partial \nu} \vartheta(\psi, r, \nu, \nu_c), \end{aligned} \tag{30}$$

which is equivalent to

$$\frac{\partial h}{\partial x} \breve{f}(x, \nu_c) + \frac{\partial h}{\partial x} \breve{g} \tau(\eta, \nu) \geq -\sigma(h(x)), \tag{31}$$

for all $(x, \nu_c) \in \mathbb{R}^2 \times D_\psi \times \mathbb{R}^3 \times \mathbb{R}^3$. By Definition 2, h is a valid CBF for (25), which combined with the fact that $\tau(\eta, \nu)$ is Lipschitz continuous and $\frac{\partial h}{\partial \nu} \neq 0$ when $(\eta, \nu) \in \partial\mathcal{C}$ guarantees forward invariance of the super-zero level set $\mathcal{C}$ from Theorem 1. □

To account for the unknown ocean current direction, Proposition 1 will be used to obtain safe controllers by specifying an upper limit on the current speed $\hat{U}_c \geq 0$ and constructing P ocean current approximations $\hat{V}_{c,i} = \hat{U}_c \operatorname{col}\left(\cos\left(\hat{\beta}_{c,i}\right), \sin\left(\hat{\beta}_{c,i}\right)\right)$, $i \in \mathcal{P} = \{1, 2, \ldots, P\}$, with evenly spaced directions $\hat{\beta}_{c,i} \in D_\psi$. Given an upper limit for the current speed $\hat{U}_c$, and a current direction $\hat{\beta}_{c,1}$ in the NED frame, we construct P ocean current approximations from

$$\hat{V}_{c,i} = R\left((i-1)\frac{2\pi}{P}\right) \hat{U}_c \begin{bmatrix} \cos(\hat{\beta}_c) \\ \sin(\hat{\beta}_c) \\ 0 \end{bmatrix}, \qquad i \in \mathcal{P}, \tag{32}$$

$$\hat{\nu}_{c,i} = R^\mathsf{T}(\psi)\hat{V}_{c,i}, \qquad i \in \mathcal{P}, \tag{33}$$

for any number of directions P divisible by 360.

Remark 1. *By specifying an upper bound on the current speed and constructing* P *evenly-spaced ocean current approximations, we are able to account for the dynamic effect that the worst possible ocean current approximation may have on some continuously differentiable function* $h(x)$ *encoding a safety-related objective. As long as the actual ocean current does not contribute to making* $h(x)$ *more negative than any of our estimates, i.e. as long as* (28) *holds,* (29) *can be enforced as a constraint on the control input and safety can be guaranteed from Proposition 1 when the linearization error from* (18) *is negligible and the control input is Lipschitz continuous.*

IV. Safety-Critical Control of ASVs

In this section we apply the results from the previous sections for safety-critical control of ASVs in the presence of ocean currents. Section IV-A defines the stabilization objectives, while Section IV-B derives ES-CLFs for position and heading control. Section IV-C describes CBF design for collision avoidance before the robust CLF-CBF-QP controller is presented in Section IV-D.

A. Stabilization Objectives

The stabilization objective is stated as a special case of the maneuvering problem [25]:

1) **Geometric Task:** For a given continuous path variable $\theta(t)$, force the configuration $\eta(t)$ to converge to the desired configuration $\eta_d(\theta)$, that is,
$$\lim_{t \to \infty} \left[\eta(t) - \eta_d(\theta(t))\right] = 0. \tag{34}$$
2) **Dynamic Task:** For a given continuous path speed $\dot{\theta}(t)$, force the configuration velocity $\dot{\eta}(t)$ to converge to a desired configuration velocity $\dot{\eta}_d(\theta(t), t)$, that is,
$$\lim_{t \to \infty} \left[\dot{\eta}(t) - \dot{\eta}_d\left(\theta(t), t\right)\right] = 0. \tag{35}$$

The primary benefit of this formulation is that design of the path and the desired motion along the path can be decoupled and approached individually in design. The desired path through K waypoints is denoted by $p_d(\theta) = \operatorname{col}\left(x_d(\theta), y_d(\theta)\right)$. This is generated using a cubic spline interpolation method as outlined in [24]. Assigning the desired heading as the angle of the tangent vector along the path $\psi_d(\theta) = \operatorname{atan2}\left(\frac{\partial y_d}{\partial \theta}, \frac{\partial x_d}{\partial \theta}\right)$ results in the desired configuration

$$\eta_d(\theta) = \operatorname{col}\left(x_d(\theta), y_d(\theta), \psi_d(\theta)\right). \tag{36}$$

We transform the desired path into a time-varying trajectory by defining a desired path speed $\dot{\theta}(t)$ according to

$$\dot{\theta} = v_d(\theta, t) := \frac{u_d(t)}{\sqrt{\left(\frac{\partial x_d}{\partial \theta}\right)^2 + \left(\frac{\partial y_d}{\partial \theta}\right)^2}}, \tag{37}$$

where $u_d(t)$ is a commanded input speed with unit $\mathrm{m/s}$. Given a piecewise constant reference speed assignment $U_r(t)$, continuous desired speed and acceleration references $u_d(t)$ and $\dot{u}_d(t)$ are obtained from the following second-order low-pass filter

$$\ddot{u}_d + 2\zeta\omega_n \dot{u}_d + \omega_n^2 u_d = \omega_n^2 U_r, \tag{38}$$

where $\zeta > 0$ is the damping ratio and $\omega_n > 0$ is the natural frequency of the filter. The desired configuration velocity and acceleration is found by differentiating (36) with respect to time

$$\dot{\eta}_d = \frac{\partial \eta_d}{\partial \theta}\dot{\theta} = \frac{\partial \eta_d}{\partial \theta} v_d(\theta, t), \tag{39}$$

$$\ddot{\eta}_d = \frac{\partial^2 \eta_d}{\partial \theta^2} v_d(\theta, t)^2 + \frac{\partial \eta_d}{\partial \theta}\left(\frac{\partial v_d}{\partial \theta} v_d + \frac{\partial v_d}{\partial t}\right). \tag{40}$$

B. Error Dynamics and Integral ES-CLFs for Stabilization

Consider the configuration error

$$y(\eta(t), \theta(t)) = \eta(t) - \eta_d(\theta(t)). \tag{41}$$

The error dynamics is found by differentiating (41) with respect to time and substituting (13)

$$\begin{aligned}
\dot{y} &= R^{\mathsf{T}}(\psi)\nu - \dot{\eta}_d(\theta, t), && (42)\\
\ddot{y} &= R^{\mathsf{T}}(\psi)\dot{\nu} + \dot{R}^{\mathsf{T}}(\psi, r)\nu - \ddot{\eta}_d(\theta, t)\\
&= R^{\mathsf{T}}(\psi)M^{-1}\left(\bar{B}(u_0)\Delta u + B(\alpha_0)\mu_0\right)\\
&\quad - R^{\mathsf{T}}(\psi)M^{-1}\left(C(\nu)\nu + D(\nu)\nu\right) + \dot{R}^{\mathsf{T}}(\psi, r)\nu - \ddot{\eta}_d\\
&= A(\psi, u_0)\Delta u + b(\psi, \nu, u_0, \theta, t). && (43)
\end{aligned}$$

In order to independently control the rate of convergence of the position and the heading angle, we let $y_1 \in \mathbb{R}^2$ and $y_2 \in D_\psi$ denote the position and heading components of the configuration error y, respectively. As discussed in Section III-D, the control model is sufficiently precise for control design provided that integral action is used in the controller to counteract the effect of the ocean currents. To this end, we define the integral states $\dot{z}_i := y_i \in \mathbb{R}^{k_i}$, where $k_i = \dim(y_i)$. The state-space representation of the error dynamics is found by defining $\xi_i := \operatorname{col}(z_i, \dot{z}_i, \ddot{z}_i) \in \mathbb{R}^{3k_i}$ and differentiating ξ_i with respect to time

$$\begin{aligned}
\dot{\xi}_i &= F_i\xi_i + G_i\left(A_i(\psi, u_0)\mu + b_i(\psi, \nu, u_0, \theta, t)\right) && (44)\\
&= \bar{f}_i(\xi_i, \psi, \nu, u_0, \theta, t) + \bar{g}_i(\psi, u_0)\Delta u, && (45)
\end{aligned}$$

for $i \in \{1, 2\}$, where A_i and b_i are the rows and elements of A and b corresponding to y_i, respectively, and

$$F_1 = \begin{bmatrix} 0 & I & 0 \\ 0 & 0 & I \\ 0 & 0 & 0 \end{bmatrix}, \qquad F_2 = \begin{bmatrix} 0 & 1 & 0 \\ 0 & 0 & 1 \\ 0 & 0 & 0 \end{bmatrix}, \tag{46}$$

$$G_1 = \begin{bmatrix} 0 & 0 & I \end{bmatrix}^{\mathsf{T}}, \qquad G_2 = \begin{bmatrix} 0 & 0 & 1 \end{bmatrix}^{\mathsf{T}}. \tag{47}$$

As alluded to in Section II, ES-CLFs will be used as they achieve fast convergence. Consider the following ES-CLF candidates for (45)

$$V_i(\xi) = \xi_i^{\mathsf{T}} P_i \xi_i, \quad i \in \{1, 2\}, \tag{48}$$

where $P_i = P_i^{\mathsf{T}}$ is positive-definite and solves the continuous-time algebraic Riccati equation

$$F_i^{\mathsf{T}} P_i + P_i F_i - P_i G_i G_i^{\mathsf{T}} P_i + Q_i = 0, \tag{49}$$

where Q_i is any positive definite matrix. Note that the symmetric and positive definite solution to (49) is guaranteed to exist since (F_i, G_i), $i \in \{1, 2\}$ is controllable [26]. The time derivative of (48) is given by

$$\dot{V}_i = \frac{\partial V_i}{\partial \xi_i}\bar{f}_i(\xi_i, \psi, \nu, u_0, \theta, t) + \frac{\partial V_i}{\partial \xi_i}\bar{g}_i(\psi, u_0)\Delta u, \tag{50}$$

where

$$\begin{aligned}
\frac{\partial V_i}{\partial \xi_i}\bar{f}_i &= \xi_i^{\mathsf{T}}\left(F_i^{\mathsf{T}} P_i + P_i F_i\right)\xi_i + 2\xi_i^{\mathsf{T}} P_i G_i b_i, && (51)\\
\frac{\partial V_i}{\partial \xi_i}\bar{g}_i &= 2\xi_i^{\mathsf{T}} P_i G_i A_i. && (52)
\end{aligned}$$

Inserting (49) results in

$$\dot{V}_i = \xi_i^{\mathsf{T}}\left(P_i G_i G_i^{\mathsf{T}} P_i - Q_i\right)\xi_i + 2\xi_i^{\mathsf{T}} P_i G_i\left(A_i\Delta u + b_i\right). \tag{53}$$

Define $\gamma_i := \frac{\lambda_{\min}(Q_i)}{\lambda_{\max}(P_i)} > 0$, where $\lambda_{\min}(\cdot)$ and $\lambda_{\max}(\cdot)$ are the minimum and maximum eigenvalues of the input matrix, respectively. It follows that $\gamma_i P_i \leq Q_i$, which yields

$$\begin{aligned}
\dot{V}_i &\leq \xi_i^{\mathsf{T}}\left(P_i G_i G_i^{\mathsf{T}} P_i - \gamma_i P_i\right)\xi_i + 2\xi_i^{\mathsf{T}} P_i G_i\left(A_i\Delta u + b_i\right)\\
&= \xi_i^{\mathsf{T}} P_i G_i\left(G_i^{\mathsf{T}} P_i \xi_i + 2\left(A_i\Delta u + b_i\right)\right) - \gamma_i \xi_i^{\mathsf{T}} P_i \xi_i. && (54)
\end{aligned}$$

Assumption 2. *The rows of the decoupling matrix $A(\psi, u_0) = R^{\mathsf{T}}(\psi)M^{-1}\bar{B}(u_0)$ are linearly independent for all $(\psi, u_0) \in D_\psi \times \mathbb{R}^{2m}$, which implies that the system is input-output feedback linearizable [27].*

Assumption 2 together with (54) implies that

$$\inf_{\Delta u \in \mathbb{R}^{2m}}\left[\frac{\partial V_i}{\partial \xi_i}\bar{f}_i + \frac{\partial V_i}{\partial \xi_i}\bar{g}_i\Delta u + \gamma_i V_i(\xi_i)\right] \leq 0, \tag{55}$$

for all $(\xi_i, \psi, \nu, u_0, \theta, t) \in \mathbb{R}^{3k_i} \times D_\psi \times \mathbb{R}^3 \times \mathbb{R}^{2m} \times \mathbb{R}_{\geq 0} \times \mathbb{R}_{\geq 0}$. Consequently, $V(\xi_i)$ is an ES-CLF for (45) with $c_1 = \lambda_{\min}(P_i)$, $c_2 = \lambda_{\max}(P_i)$ and $c_3 = \gamma_i$. Note that the rate of exponential convergence γ_i can be controlled through the positive-definite matrix Q_i.

C. CBFs for Collision Avoidance with Static Obstacles

To achieve collision avoidance, we will employ Proposition 1, and the ocean current estimation procedure in Section III-D to obtain CBFs for the ASV model (13) without knowledge of the true ocean current. We only consider static obstacles, and refer to [19] for collision avoidance of dynamic obstacles using CBFs. The model (23) combined with (15) and (18) in state-space form is given by

$$\dot{x} = f(x) + g\Delta u + \begin{bmatrix} 0 \\ \vartheta(x, \nu_c) \end{bmatrix}, \tag{56}$$

where $x = \operatorname{col}(\eta, \nu)$ and the expressions for $f(x)$ and g are given in Section III-C. Consider a spherical obstacle with radius $r_{\text{obs}} > 0$. A scalar distance measure between the obstacle and the body-fixed vessel frame is

$$d(x_1) = \sqrt{\left(p^n_{\text{obs}} - p^n\right)^{\mathsf{T}}\left(p^n_{\text{obs}} - p^n\right)} - r_{\text{obs}}. \tag{57}$$

where $p^n_{\text{obs}} \in \mathbb{R}^2$ is the position of the center of the obstacle in the NED frame. Enforcing the positivity of the following continuously differentiable function will avoid collisions [17]

$$h(x) = d(x_1) + k\dot{d}, \tag{58}$$

where $k > 0$ and $\dot{d} = \frac{\partial d}{\partial x_1}R(x_1)x_2 := J(x_1)x_2$. Differentiating h with respect to time yields

$$\begin{aligned}
\dot{h} &= \frac{\partial h}{\partial x}f(x) + \frac{\partial h}{\partial x}g\Delta u + \frac{\partial h}{\partial x_2}\vartheta(x, \nu_c) && (59)\\
&= J(x_1)\left(x_2 + k\vartheta(x, \nu_c)\right) + k\dot{J}(x_1, x_2)x_2\\
&\quad + kJ(x_1)M^{-1}\left(\bar{B}(u_0)\Delta u + B(\alpha_0)\mu_0 - C(x_2)x_2 - D_l x_2\right). && (60)
\end{aligned}$$

D. Safety-Critical Control via Quadratic Programming

In summary, the stabilization objectives consist of position and heading control encoded by the integral ES-CLFs $V_1(\xi_1)$ and $V_2(\xi_2)$, while the safety-related collision avoidance objective is encoded by the continuously differentiable function $h(x)$. The CLF-CBF-QP from Section II-C is modified for an ASV with a nonlinear actuator model as follows

$$\underset{(\Delta u,\delta)\in\mathbb{R}^{2m+2}}{\text{minimize}} \; \Delta u^{\mathsf{T}}\left(H+\Omega\right)\Delta u + 2u_0^{\mathsf{T}} H \Delta u + \delta^{\mathsf{T}} W \delta \tag{61a}$$

subject to

$$\frac{\partial V_1}{\partial \xi_1}\bar{f}_1 + \frac{\partial V_1}{\partial \xi_1}\bar{g}_1 \Delta u \leq -\gamma_1 V_1(\xi_1) + \delta_1, \tag{61b}$$

$$\frac{\partial V_2}{\partial \xi_2}\bar{f}_2 + \frac{\partial V_2}{\partial \xi_2}\bar{g}_2 \Delta u \leq -\gamma_2 V_2(\xi_2) + \delta_2, \tag{61c}$$

$$\frac{\partial h}{\partial x} f(x) + \frac{\partial h}{\partial x} g \Delta u \geq -\sigma(h(x)) - \min_{i\in\mathcal{P}} kJ(x_1)\varphi_i(x), \tag{61d}$$

$$\mu_{\min} - \mu_0 \leq \Delta\mu \leq \mu_{\max} - \mu_0, \tag{61e}$$

$$T\Delta u_{\min} \leq \Delta u \leq T\Delta u_{\max}, \tag{61f}$$

where $H = \mathrm{diag}(H_1, 0) \in \mathbb{R}^{2m\times 2m}$ penalizes the force magnitudes squared, while $\Omega \in \mathbb{R}^{2m\times 2m}$ is a diagonal matrix penalizing the squared rate of change of the force magnitude and azimuth angle control inputs, and $(\delta_1, \delta_2) \in \mathbb{R}^2$ are slack variables penalized by the diagonal weighting matrix $W \in \mathbb{R}^{2\times 2}$. Moreover, $\mu_{\min}$ and $\mu_{\max}$ are the negative and positive force magnitude constraints, T is the sampling time, and $\Delta u_{\min}$ and $\Delta u_{\max}$ are the negative and positive rate constraints, respectively. For practical purposes, it is beneficial to include magnitude and rate constraints in the QP controller as demonstrated in [10], at the expense of guaranteed Lipschitz continuous solutions to the QP.

V. Numerical Simulation

In this section we verify the theoretical developments from the previous sections through simulation of a double-ended autonomous passenger ferry [28]. In terms of actuators, the ferry is equipped with two azimuth thrusters and the simulation model consists of (13) with a realistic thruster model for (15) taking thruster force deadband, magnitude and rate constraints, and azimuth angle magnitude and rate constraints into account. Note that the simulation model includes nonlinear damping, which is not accounted for in the CLF or CBF design. The ES-CLF parameters are given by $Q_1 = \mathrm{diag}\left(0.01I_2, 200I_2, 400I_2\right)$ and $Q_2 = \mathrm{diag}\left(0.1, 400, 800\right)$, where I_2 is the 2×2 identity matrix. The remaining parameters are summarized in Table I. Following the procedure outlined in Section III-D, P evenly spaced ocean current approximations are constructed from (32)–(33). The dynamic effect of the worst-case ocean current is therefore approximated by the P continuous maps given by (27). Note that our choice of $\hat{\beta}_c$ is the worst possible guess, since each direction is separated by 30°, resulting in a 15° offset between the actual current direction and the best estimate(s).

Simulation results are shown in Figs. 1 to 3 and 5, where simulations with and without the robustifying term in (61d), (i.e. assuming $\varphi = 0$, $i \in \mathcal{P}$) are depicted in Figs. 1 and 5.

TABLE I

Control Parameters

Param.	Value	Param.	Value	Param.	Value
P	12	r_{obs}	13 m	H_1	$0.5I_2$
β_c	$-60°$	$\sigma(h)$	ϕh	Ω_1	$0.0001I_2$
$\hat{\beta}_c$	15°	ϕ	0.1	Ω_2	$2500I_2$
U_c	1 m/s	k	$\frac{20}{3}$	W	$1.5\cdot 10^4 I_2$
$\hat{U}_c$	1.1 m/s	$\mu_{\min}$	-293 N	$\mu_{\max}$	500 N
T	0.01 s	$\Delta\mu_{\max}$	160 N/s	$\Delta\mu_{\min}$	$-\Delta\mu_{\max}$
		$\Delta\alpha_{\max}$	30 deg/s	$\Delta\alpha_{\min}$	$-\Delta\alpha_{\max}$

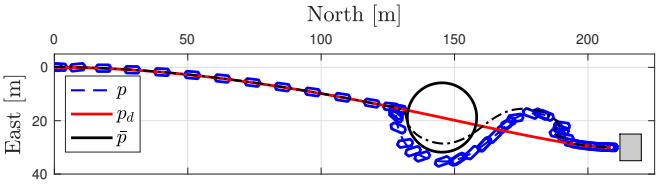

Fig. 1. North-East plot showing the path p, the desired path p_d, the heading and the spherical obstacle. The black dash-dotted line $\bar{p}$ represents the path followed by the ASV when omitting the robustifying last term in (61d).

From Figs. 1 and 5, it is clear that the non-robust CBF candidate fails to achieve forward invariance of the super-zero level set of (58), resulting in a collision. Observe from Fig. 4 that both thrusters are in maximum positive saturation from $t \approx 170$ s to $t \approx 182$ s due to the strict penalty on non-zero slack variables and by using a linear $\mathcal{K}_\infty$ function in (61d). Moreover, the system exhibits excessively large tracking errors at $t \approx 190$ s because of the incompatibility between the collision avoidance and stabilization tasks, combined with the significant size of the spherical obstacle. Nevertheless, the system remains stable and successfully catches up with the reference trajectory. The overshoot in Figs. 1 and 2 occurs due to the ocean current pushing the ship westward while the integral action saturates from attempting to recover from a significant tracking error. Improved transient behavior after avoiding a collision can be achieved by employing anti-wind up techniques and/or trajectory replanning if the positional tracking error exceeds some threshold. With the exception of poor transient performance due to successfully avoiding a collision, the integral ES-CLFs contribute to successful tracking of the configuration and velocity references as seen in Figs. 2 and 3.

VI. Conclusions and Future Work

This paper has presented an optimization-based framework for safety-critical control of ASVs with robustness guarantees in the presence of unknown ocean currents. The framework is holistic in the sense that it solves the problems of stabilization, reactive collision avoidance and control allocation in a unified manner. Conditions ensuring forward invariance of the super-zero level set of continuously differentiable functions have been derived for a class of uncertain nonlinear systems. These conditions can be employed to ensure safety in the presence of unknown system nonlinearities. Moreover, we have specialized these conditions for an ASV subject to unknown ocean currents to obtain robust CBFs providing collision avoidance guarantees. Furthermore, the control allocation problem has been unified with the control problem by linearizing the actu-

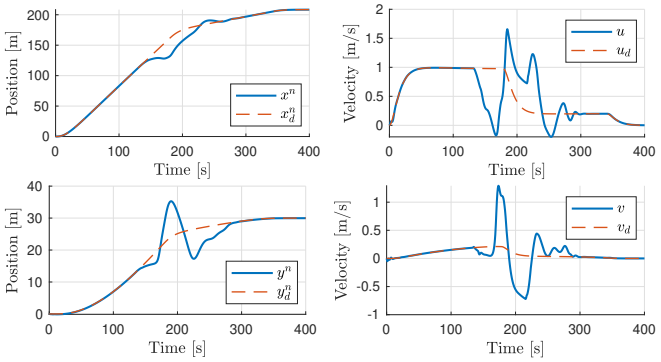

Fig. 2. The actual and desired North and East positions x^n, y^n and x_d^n, y_d^n, and the actual and desired surge u, u_d and sway v, v_d velocities.

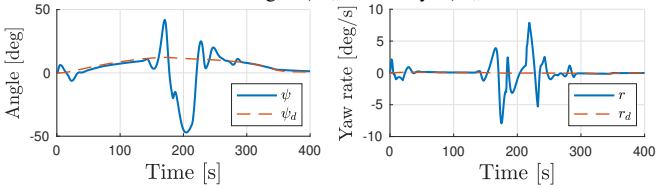

Fig. 3. The actual and desired heading angle ψ and ψ_d and the actual and desired yaw rate r and r_d.

ator configuration matrix at every sampling instant to avoid a non-convex optimization problem, enabling constraints on the control input to be explicitly accounted for in the motion controller. This unification helps avoid instability due to actuator saturation. Additionally, we have incorporated integral action into CLFs encoding stabilization objectives. The framework has been verified through simulation for a double-ended passenger ferry, where successful tracking of a time-varying trajectory and reactive collision avoidance has been demonstrated. Future work is aimed at full-scale experiments of the proposed framework for a double-ended passenger ferry.

REFERENCES

[1] Autonomous Shipping Initiative for European Waters (AUTOSHIP). (2020). [Online]. Available: https://cordis.europa.eu/project/id/815012

[2] Norwegian SciTech News. (2018) Driverless ferries to replace footbridges. [Online]. Available: https://norwegianscitechnews.com/2018/06/driverless-ferries-to-replace-footbridges/

[3] A. Orthmann and A. Ziegwied, "The force multiplier effect using autonomous surface vessels for hydrographic survey in the arctic," in *OCEANS 2017*, Anchorage, AK, USA, Sep. 2017, pp. 1–4.

[4] T. A. Johansen, T. I. Fossen, and S. P. Berge, "Constrained nonlinear control allocation with singularity avoidance using sequential quadratic programming," *IEEE Trans. Control Syst. Technol.*, vol. 12, no. 1, pp. 211–216, Jan. 2004.

[5] A. Veksler, T. A. Johansen, F. Borrelli, and B. Realfsen, "Cartesian thrust allocation algorithm with variable direction thrusters, turn rate limits and singularity avoidance," in *Proc. 2014 IEEE Conf. Control Applications*, Antibes, France, Oct 2014, pp. 917–922.

[6] T. A. Johansen and T. I. Fossen, "Control allocation – a survey," *Automatica*, vol. 49, pp. 1087–1103, May 2013.

[7] A. Veksler, T. A. Johansen, F. Borrelli, and B. Realfsen, "Dynamic positioning with model predictive control," *IEEE Trans. Control Syst. Technol.*, vol. 24, no. 4, pp. 1340–1353, July 2016.

[8] A. Ames and M. Powell, "Towards the unification of locomotion and manipulation through control Lyapunov functions and quadratic programs," *Control of Cyber-Physical Systems*, pp. 219–240, 2013.

[9] A. D. Ames, K. Galloway, K. Sreenath, and J. W. Grizzle, "Rapidly exponentially stabilizing control Lyapunov functions and hybrid zero dynamics," *IEEE Trans. Autom. Control*, vol. 59, no. 4, pp. 876–891, Apr. 2014.

[10] K. Galloway, K. Sreenath, A. D. Ames, and J. W. Grizzle, "Torque saturation in bipedal robotic walking through control Lyapunov function-based quadratic programs," *IEEE Access*, vol. 3, pp. 323–332, 2015.

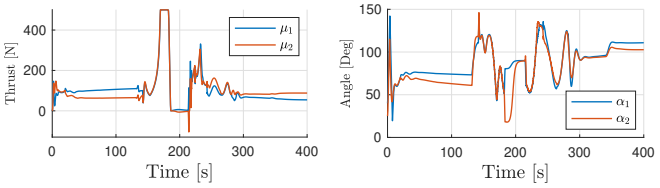

Fig. 4. The thruster and azimuth angle control inputs, μ and α, respectively.

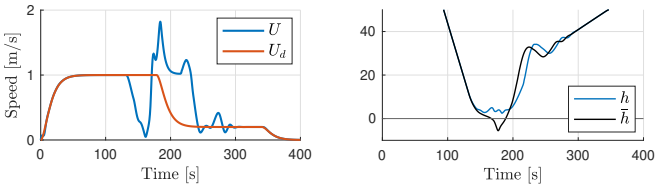

Fig. 5. Actual and desired speed U and U_d, and the function h when the last term in (61d) is included, h, and omitted, $\bar{h}$, respectively.

[11] Q. Nguyen and K. Sreenath, "Optimal robust control for constrained nonlinear hybrid systems with application to bipedal locomotion," in *Proc. 2016 American Control Conf.*, Boston, MA, USA, Jul. 2016.

[12] A. D. Ames, J. W. Grizzle, and P. Tabuada, "Control barrier function based quadratic programs with application to adaptive cruise control," in *Proc. 53rd IEEE Conf. Decision and Control*, Los Angeles, CA, USA, Dec. 2014.

[13] E. A. Basso and K. Y. Pettersen, "Task-priority control of redundant robotic systems using control Lyapunov and control barrier function based quadratic programs," in *Proc. 21st IFAC World Congress*, Berlin, Germany, Jul. 2020.

[14] Y. Wang and S. Boyd, "Fast evaluation of quadratic control-Lyapunov policy," *IEEE Trans. Control Syst. Technol.*, vol. 19, no. 4, pp. 939–946, 2010.

[15] P. Wieland and F. Allgöwer, "Constructive safety using control barrier functions," *IFAC Proc. Volumes*, vol. 40, no. 12, pp. 462–467, 2007.

[16] M. Z. Romdlony and B. Jayawardhana, "Uniting control Lyapunov and control barrier functions," in *Proc. 53rd IEEE Conf. Decision and Control*, Los Angeles, CA, USA, Dec. 2014.

[17] U. Borrmann, L. Wang, A. D. Ames, and M. Egerstedt, "Control barrier certificates for safe swarm behavior," *IFAC-PapersOnLine*, vol. 48, no. 27, pp. 68 – 73, 2015.

[18] Y. Emam, P. Glotfelter, and M. Egerstedt, "Robust barrier functions for a fully autonomous, remotely accessible swarm-robotics testbed," in *Proc. 58th IEEE Conf. Decision and Control*, Nice, France, Dec. 2019.

[19] E. H. Thyri, E. A. Basso, M. Breivik, K. Y. Pettersen, R. Skjetne, and A. M. Lekkas, "Reactive collision avoidance for ASVs based on control barrier functions," in *Proc. 4th IEEE Conf. Control Technol. and Applications*, Montreal, Canada, Aug. 2020.

[20] T. Gurriet, A. Singletary, J. Reher, L. Ciarletta, E. Feron, and A. Ames, "Towards a framework for realizable safety critical control through active set invariance," in *Proc. 2018 ACM/IEEE 9th International Conference on Cyber-Physical Systems*, Porto, Portugal, April 2018, pp. 98–106.

[21] A. D. Ames, X. Xu, J. W. Grizzle, and P. Tabuada, "Control barrier function based quadratic programs for safety critical systems," *IEEE Trans. Autom. Control*, vol. 62, no. 8, pp. 3861–3876, Aug. 2017.

[22] A. D. Ames, S. Coogan, M. Egerstedt, G. Notomista, K. Sreenath, and P. Tabuada, "Control barrier functions: Theory and applications," in *Proc. 2019 European Control Conference*, Naples, Italy, Jun. 2019.

[23] T. I. Fossen, *Handbook of Marine Craft Hydrodynamics and Motion Control*. Wiley, 2011.

[24] R. Skjetne, "The maneuvering problem," Ph.D. dissertation, Norwegian University of Science and Technology, 2005.

[25] R. Skjetne, T. I. Fossen, and P. V. Kokotović, "Robust output maneuvering for a class of nonlinear systems," *Automatica*, vol. 40, no. 3, pp. 373 – 383, 2004.

[26] J. Willems, "Least squares stationary optimal control and the algebraic riccati equation," *IEEE Trans. Autom. Control*, vol. 16, no. 6, pp. 621–634, December 1971.

[27] A. Isidori, *Nonlinear Control Systems*, 3rd ed. Springer, 1995.

[28] A. A. Pedersen, "Optimization based system identification for the milliAmpere ferry," Master's thesis, Norwegian University of Science and Technology (NTNU), Trondheim, Norway, 2019.